Manipulating cold atoms with optical fibres

Shrabana Chakrabarti*

Applied Nuclear Physics Division, Saha Institute of Nuclear Physics, 1/AF Bidhanager, Kolkata 700 064, India

In this article we present some demonstrations of atom–photon interactions at low photon level using optical fibres. We report an experiment on the interaction between cold atoms produced in a magneto optical trap and tapered optical nanofibre and discuss some applications of the same. We then expound our experimental plan to study nonlinear processes such as electromagnetically induced transparency in laser cooled atomic medium confined within a hollow core photonic crystal fibre. Possible applications of this system are also discussed.

Introduction

EFFICIENT processing of information is of major importance in our modern society. Conventional electronic data storage and processing, based on two-state (0, 1) binary form, is about to reach its limits in terms of capacities and processor speeds. Thus, there is an urgent need to find novel approaches to store and process large amounts of information. One such extremely promising approach is based on quantum information processing (QIP) that uses quantum bits (qubits) that have infinitely many quantum states that can be exploited to obtain a more powerful information platform.

Experimental realization of qubits is one of the main challenges in QIP. Photons (or other quantum states of light) can be considered as good choice for qubits, specially for communication. Large storage capacity and stable quantum memory[1–8] are very critical for the realization of QIP[9], such as in quantum communication[10–12] and quantum computation[13]. Two important factors of QIP namely storage and memory, depend mostly on strong atom–photon interactions. One process of initiating strong atom–photon interactions could be by tightly confining light. Tight confinement of light leads to an increase in the electric field amplitude of single photons which results in increased atom–light interactions. Confinement of light was observed in various systems such as high-Q optical microresonators[14,15], semiconductor waveguides[16,17], tapered optical fibres[18–20], and hollow core photonic crystal fibres (PCFs)[21]. Tapered optical

fibres (TOF) and hollow core photonic crystal fibres (HCPCF) can be considered as two great tools, based on the most promising fibre technology, that pave way for cutting edge research on studies of strong atom–photon interactions at low light levels. It was demonstrated by Kato and Aoki[22] that trapped atoms could be coupled to a fibre-based optical cavity, where the cavity is produced by splicing an optical nanofibre (ONF) between two fibre-Bragg grating mirrors. The potential of ONFs as efficient tools for quantum technological advances was quite evident from this experiment. HCPCF provides strong transverse confinement of light and atoms that are trapped within its hollow core and could lead to large and controlled atom–photon interactions. Atom–photon interactions based on both these fibre optical techniques will be discussed in this article. We will primarily concentrate on the interaction between cold neutral atoms and light mediated by these two types of fibres namely tapered optical nanofibre (TNF) and HCPCF.

Atom–light coupling in tapered optical nanofibres

Heat and pull technique is usually employed to fabricate an optical nanofibre. A standard optical fibre is first stripped of its acrylic coating. It is then heated to a very high temperature close to melting point of glass. This renders the fibre to be in a plastic regime which enables it to be elongated without breaking. When the fibre is pulled, it elongates leading to a gradual reduction in its diameter producing three main regions as shown in Figure 1. These are, pigtail, taper or transition region and the waist. When the waist is sufficiently small, light passing through the fibre will generate significant evanescent field outside the fibre[23].
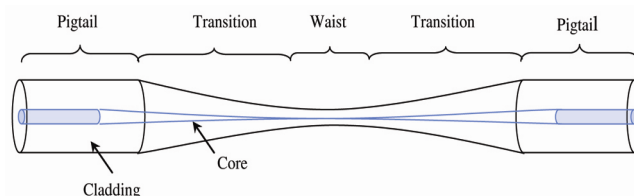
Figure 1. Schematic diagram of the parts of a tapered optical nanofibre (TNF). It consists of three main parts: pigtail, which is an unchanged region of the standard fibre, taper or transition region where the core size gradually shrinks, and the waist, where the core completely vanishes forcing the guided light to create an evanescent field outside the fibre.

Study of nonlinear phenomena in an atomic medium usually requires large light intensities and tightly focused laser beams. Tight focusing of light however imposes a restriction on its interaction region which is defined by Rayleigh length, L_R, given by $L_R = \pi w_0^2 / \lambda$, where w_0 is beam waist at the narrowest point and λ is the laser wavelength. In TNFs a strong evanescent field is created at its waist which contains most of the power from light launched into the fibre[24]. Hence TNFs help in overcoming the limitation[25] due to Rayleigh length of focused beams. The evanescent field of the TNFs may interact with atoms in its vicinity[26] and fluorescence from excited atoms can preferentially couple into nanofibre-guided modes[27,28]. These properties of TNFs make them suitable candidates for integration into cold atomic systems facilitating the study of strong atom–photon interactions.

In this article we discuss an experiment where the fluorescence due to spontaneous emission from cold atomic rubidium cloud couples into the guided modes of a TNF. It proves that TNFs are potential tools that can be used for determining various MOT parameters like cloud diameter and MOT lifetime, when the number of atoms trapped in a MOT is not too large.

Experimental arrangement

A basic MOT set-up[29,30] was used to create a cold cloud of ^{85}Rb atoms near the waist region of TNF[31]. Three pairs of mutually perpendicular, opposite circularly polarized and retroreflecting laser beams, all intersecting at a point produce optical force necessary for cooling the atoms. The cooling laser is locked red detuned from $5S_{1/2}$ $F = 3 \rightarrow 5S_{3/2}$ $F' = 4$ closed cycle transition (Figure 2). A repumper laser is locked to $5S_{1/2}$ $F = 2 \rightarrow 5P_{3/2}$ $F' = 3$ transition (Figure 2). A pair of anti-Helmholtz coils generate a quadrupole magnetic field, the centre of which
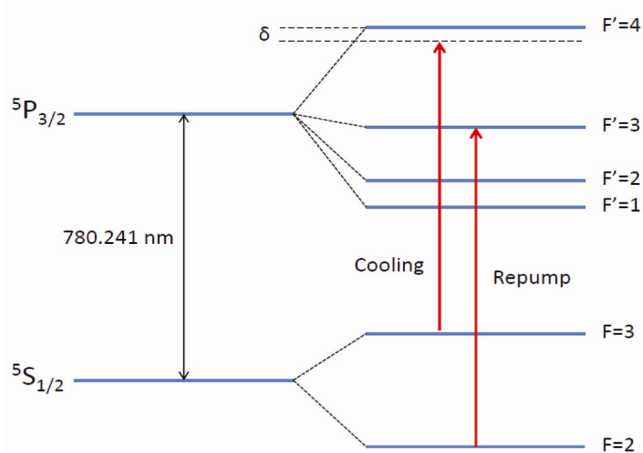
Figure 2. Schematic energy level diagram of ^{85}Rb showing cooling and repumping laser fields.

coincides with the point of intersection of laser beams, to produce MOT necessary to confine the cold atoms. The cold cloud is viewed orthogonally using charge coupled device (CCD) cameras. The TNF is mounted inside an ultra-high vacuum MOT chamber using electrical feedthroughs attached to a vacuum flange. Tapered region of the fibre is held in an U-shaped mount, ensuring that the thinnest section of the fibre is centred in MOT chamber[31]. Other than anti-Helmholtz coils, pairs of smaller coils are also used to spatially overlap the cold cloud with the waist region of TNF. As a result of this overlap with TNF waist, the cold cloud becomes cigar-shaped with a $1/e$ vertical length of 2 mm and a horizontal length of 1.3 mm, and an average MOT density of 4×10^6 atoms/mm^3. Light fluorescing from cold atoms placed close to fibre waist, couples into the guided modes of the fibre and is detected by a single photon counting module (SPCM, Perkin Elmer) attached to one end of the fibre. When SPCM receives a photon, a transistor–transistor logic (TTL) pulse is sent to a counter (Hamamatsu counting unit) whose data is recorded on a computer.

Results and discussion

Fluorescence detection

The efficiency of TNF to couple fluorescent light from cold atoms placed close to its waist region was studied first. The coupling efficiency of TNF was studied by monitoring the photon count on SPCM during stepwise switching on and off the various elements producing MOT[31]. During MOT loading sequence, first the repumper laser was switched on, followed by cooling laser and finally the magnetic field was switched on. It was found that the initial count rate was 1.5×10^4 s^{-1} in the absence of any optical and magnetic fields. It can also be accounted to darkcount of the detector and various light sources in the laboratory. When the repumper field is switched on, the count rate increases to 2×10^4 s^{-1}. A further increase of 4×10^4 s^{-1} is observed in the presence of cooling laser beams. Finally when the magnetic field is turned on, the actual MOT loading occurs resulting in a dramatic increase of 4×10^5 s^{-1}. This observation confirms that the photon counts result due to coupling of fluorescence from cold cloud into the guided modes of TNF.

The efficiency of fluorescence from cold atoms coupled into TNF is influenced by van der Waals interactions between atoms and the dielectric surface of TNF. Van der Waals interactions were manifested in the frequency-dependent fluorescence power coupled from atom cloud into TNF. These interactions lead to a pronounced asymmetry in the lineshape of the coupled fluorescence spectrum[32]. It was observed that this asymmetry increased

when the atom cloud around TNF was more compact and also when the radius of TNF was increased[32]. Asymmetry occurs due to bound–bound transitions of the ground and excited state van der Waals potentials.

MOT profile, loading and decay

To determine the size of MOT, the cold cloud of Rb atoms is moved across the waist of TNF and the resulting photon count is recorded as a function of the position of TNF. A CCD in combination with a telescope is used to monitor the movement of cold cloud. The pixels of CCD are calibrated in units of length. When one of the edges of cloud overlaps with TNF, fluorescence from the cold cloud near the fibre surface gets coupled into its guided modes. As MOT centre comes in close proximity of TNF waist, the fluorescence count rate enhances. The count rate decreases as the cloud moves away from the fibre. By measuring the change of photon count rate as a function of cloud position, cloud shape and atom density are determined. Figure 3 gives a graphical representation of photon counts from TNF as a function of the position of TNF with respect to the cloud.

To determine MOT loading with time, a Rb dispenser placed inside the vacuum chamber is resistively heated. The number of atoms in a MOT is proportional to fluorescence intensity emitted from them. MOT loading is studied using two techniques – in the first technique fluorescence from the entire MOT is focused onto a photodiode and the output voltage is measured. By observing the change in this voltage, an instantaneous time evolution of MOT loading is understood. In the second method, it is considered that the loading of atoms in MOT centre, near TNF waist, is a function of the entire MOT loading. Hence MOT loading rate is determined by monitoring the fluorescence from MOT coupling into TNF.
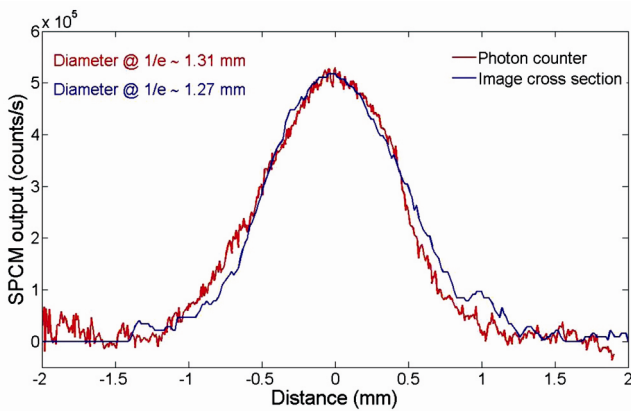
MOT lifetime is also similarly measured by switching off the Rb dispenser and recording the decrease in photon count with time. This happens due to decay in the number of trapped atoms, since loss rate from trap exceeds the capture rate. By studying this decay, lifetime of the trap is determined. Standard photodiode and TNF techniques are both employed to measure MOT decay time as well. Figure 4 shows the lifetime of trapped atoms as a function of time using standard technique as well as TNF method.
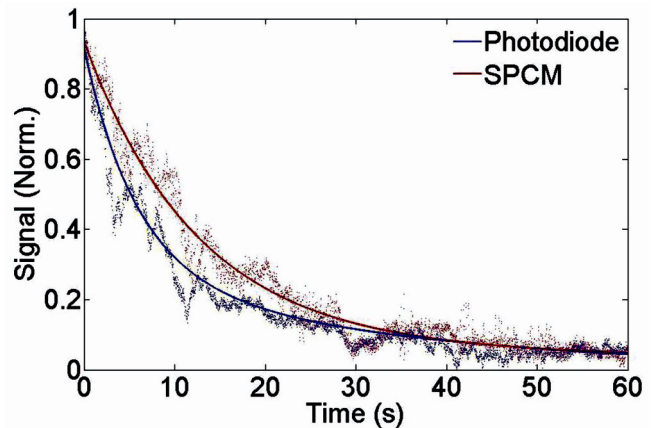
The temperature of the atom cloud is estimated using a technique of forced oscillations[33]. A one-dimensional oscillatory motion is imparted to MOT by modulating the current of MOT coils. This results in sinusoidal oscillations of the cold atom cloud causing a sinusoidal variation in cloud's density. Oscillation of the cold cloud around TNF generates sinusoidal variations in the count rate of photons detected by SPCM attached to one end of the fibre. From the output of SPCM, the natural frequency of oscillation is obtained which gives the value of spring constant (κ) from the relation, $\kappa = m\omega_n^2$, where m is mass of the atomic sample and ω_n is the oscillation frequency. The cloud temperature is estimated from the relation

$$k_B T = \kappa \langle r_x^2 \rangle, \tag{1}$$

Where k_B is the Boltzmann constant, T is the cloud temperature and $\langle r_x^2 \rangle$ is $1/e^2$ radius of the oscillating atom cloud.

Conclusion

It can be concluded from our results that TNF could serve as a suitable technique for determining MOT characteristics when the trapped atom number is small. TNFs can be

Figure 3. Determination of cloud profile using TNF technique (red curve) and CCD camera (blue curve). $1/e$ diameter of the cold cloud was found to be 1.31 (± 0.38) mm using TNF technique and 1.27 (± 0.25) mm using the standard CCD technique.

Figure 4. MOT decay curve as observed by photodiode (blue curve) and TNF method (red curve). $1/e$ lifetime of the MOT was found to be $\tau = 9.4$ (± 0.47) sec using photodiode technique and $\tau = 13$ (± 0.68) sec using the TNF technique.
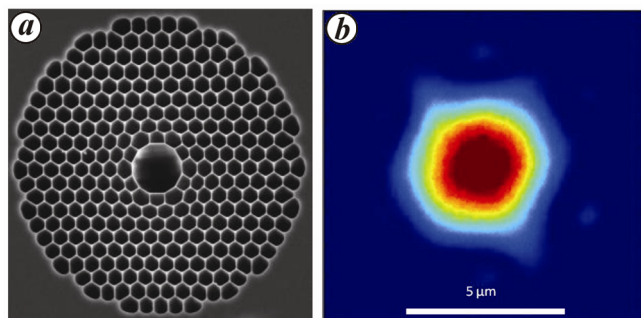
efficiently used for manipulating cold atoms and have great potential as tools for probing cold atomic clouds.

Guiding cold atoms inside HCPCF

Hollow core optical fibres can guide and confine both atoms and light. There have been reports of atom guiding inside hollow fibre using optical dipole traps (ODTs)[33–37]. These experiments used capillaries to guide light in multiple modes of cladding or core. Such fibres generate inhomogeneous fields resulting in uncontrolled guiding, heating and loss due to lack of efficient confinement. Photonic crystal fibres on the contrary propagate a single Gaussian mode confined to a hollow core[21,38]. HCPCF are a special class of optical fibres that use a micro-structured cladding region with air holes to guide light into a hollow core. Figure 5 *a* shows an image of such a fibre observed by a scanning electron microscope (SEM) and Figure 5 *b* gives the near field intensity profile of HCPCF. Light is guided inside the hollow core using photonic band-gap effect. Cold atoms loaded into a Gaussian mode of HCPCF can be confined and controllably guided along the fibre using an optical guide. There have been successful manifestations of trapping ultra-cold atoms[39] or guiding thermal[40] or laser-cooled atoms[41] through hollow core photonic band gap fibres. These fibres can also be used for spectroscopy[42,43] and gas sensing experiments[44] by filling the hollow core with atomic or molecular gases. In our approach we intend to create an optically dense medium of cold Rb atoms confined within a hollow core photonic crystal to facilitate the study of atom–photon interactions at low photon levels. The confinement of cold atoms prevents atom-wall collisions inside the fibre core. The use of laser cooled atoms ensures a significant reduction in Doppler width.

Experimental arrangement

The experimental apparatus consists of a piece of single-mode HCPCF vertically mounted inside an ultra-high vacuum chamber. A cold cloud of ^{85}Rb atoms generated in a MOT, focused with a magnetic guide, will be loaded into the hollow core of PCF. A red detuned dipole trap formed by a single laser beam guided through the fibre will be used to radially confine the atoms inside the fibre. Owing to the small diameter of the guided mode, a strong transverse confinement and deep trapping potential is expected at guiding light intensities of a few milliwatts. Atoms inside the fibre will be probed by monitoring the transmission of a very low intensity (~ few pW) probe beam coupled into single mode HCPCF by a single-photon counter.

Magneto optical trap arrangement to generate a source of cold atoms

A standard MOT for ^{85}Rb atoms is produced. The cooling laser beams are generated from a frequency stabilized external cavity diode laser (ECDL) and locked red detuned from $5S_{1/2}$ $F = 3 \rightarrow 5P_{3/2}$ $F' = 4$ closed transition using Doppler-free saturated absorption spectroscopy (Figure 2). The cooling laser is split suitably to generate three pairs of mutually perpendicular, opposite circularly polarized and retro-reflecting beams that intersect at the centre of an ultra-high vacuum chamber. The repumping laser field produced by another ECDL is locked to $5S_{1/2}$ $F = 2 \rightarrow 5P_{3/2}$ $F' = 3$ transition of ^{85}Rb (Figure 2). The magnetic field required to trap cold atoms is realized by two circular coils operating in an anti-Helmholtz configuration such that the zero field coincides with the point of intersection of all the six laser beams. After completion of MOT loading, the magnetic quadrupole trap will be switched off. In addition, a magnetic funnel is created by four current-carrying Kapton coated copper wires. These wires are held tightly and parallel to HCPCF by a cylindrical mount. The wires fan out upwards outside the mount in an upside-down pyramid structure above the fibre tip. When current is sent through wires, a transverse quadrupole field is generated such that its gradient increases with decreasing distance to the fibre. All magnetic fields will be turned off after atoms are transferred to the fibre. An optical dipole trap beam at 800 nm (with power ~30 mW) will then be sent through the fibre to confine and guide the trapped atoms. The presence of atoms inside HCPCF will be given by absorption spectrum of a probe beam sent through the HCPCF.

Design of anti-Helmholtz coils

A magnetic field gradient required to produce a stable cold cloud is between 10 and 11 Gauss/cm. It can be estimated from Biot Savart Law (eq. 2) that gives the magnetic field produced by a pair of circular coils at a distance x from the centre[45]. Considering the number of turns, $n = 170$, radius of each coil, $a = 7.75$ cm, distance

Figure 5. *a*, SEM image of HCPCF, *b*, Near field intensity profile of HCPCF.

between the two coils to be $d = 15.5$ cm and the current passing through each coil to be $I = 6.0$ Amp, we simulated a magnetic field gradient generated by the coils using a Matlab code

$$B = \frac{\mu_0 n I a^2}{2(a^2 + x^2)^{3/2}},\qquad (2)$$

In eq. (2), μ_0 is the free space permeability. Equation (2) gives magnetic field in only one dimension whereas Matlab code simulates the results in 3D as well. The resulting magnetic field in the x–y plane is given in Figure 6 a and the magnetic field gradient along z-axis is presented in Figure 6 b. We estimated a field gradient of 10.8 Gauss/cm.

Design of fibre mount for HCPCF

In order to load and guide cold atoms from MOT into HCPCF, a suitable ultra-high vacuum compatible fibre
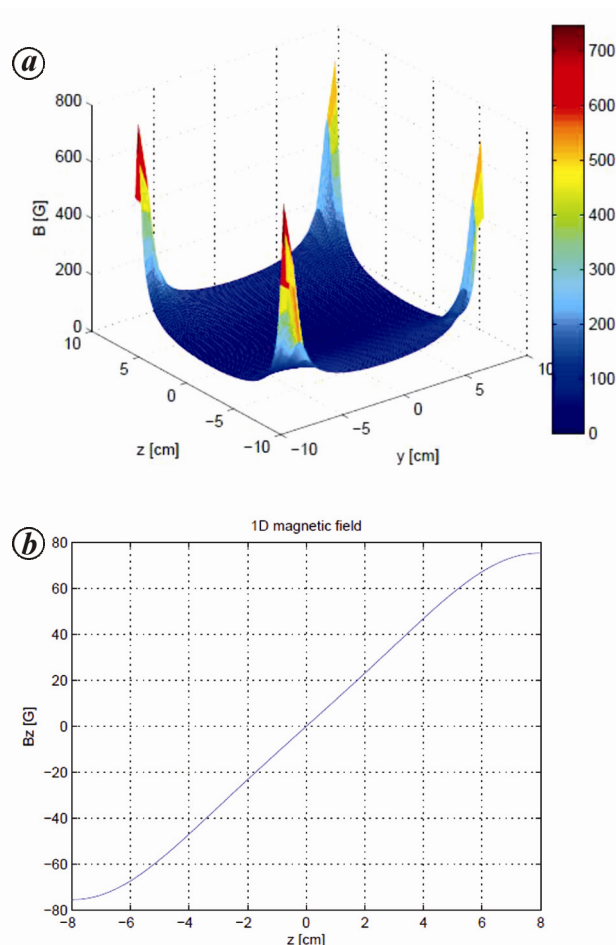
Figure 6. *a*, Magnetic field in 2D plane namely *x*–*y* plane, *b*, 1D magnetic field along *z*-axis.

mount has to be designed. We designed our fibre mount using Autodesk Inventor software. The mount is used to hold HCPCF vertically within MOT chamber such that the fibre tip is about 5 mm below the position of cold cloud. The fibre mount assembly will then be attached to a bottom CF 35 port of MOT chamber through a CF 35–CF 16 zero length adaptor. A CF 16 viewport will be attached to zero length adaptor for the entry of one of the cooling beams as well as for dipole trap beam. HCPCF will be held tightly in position by four Kapton coated copper wires that run parallel to the fibre and fan outwards like an inverted pyramid structure producing the magnetic guide. In addition to these, the fibre mount contains two tightly focusing lenses for dipole trap beam.

Experimental plan and its applications

We propose to demonstrate the phenomenon of electromagnetically induced transparency (EIT) in cold atoms trapped within a HCPCF. To demonstrate EIT, the atoms will first be prepared in $F = 2$ ground state. A linearly polarized probe tuned to D2 $F = 2 \rightarrow F' = 2$ transition will be used to probe the medium. The probe beam will be weak (~ 100 pW) and propagate through HCPCF vertically along the direction of one of the cooling beams, and then detected by the photon counter. Under this condition, the medium will be completely opaque at resonance. A co-propagating control field resonant with $F = 3 \rightarrow F' = 2$ transition, will render the atomic ensemble transparent near the probe resonance. The resulting EIT will lead to a steep dispersion and slowing of group velocity of the medium that will generate delayed probe pulses passing through it. When EIT is formed we will adiabatically switch off the strong control field. Under this condition, probe pulse will be stopped and a stationary spin excitation will be generated. The probe pulse can be recovered by reapplying the control field.

This type of system could be used to realize stationary light pulses (SLPs), few photon controlled all-optical switch and some important elements of QIP.

1. Chanelière, T., Matsukevich, D. N., Jenkins, S. D., Lan, S. Y., Kennedy, T. A. B. and Kuzmich, A., Storage and retrieval of single photons transmitted between remote quantum memories. *Nature*, 2005, **438**, 833–836.
2. Eisaman, M. D., Andrè, A., Massou, F., Fleischhauer, M., Zibrov, A. S. and Lukin, M. D., Electromagnetically induced transparency with tunable single-photon pulses. *Nature*, 2005, **438**, 837–841.
3. Choi, K. S., Deng, H., Laurat, J. and Kimble, H. J., Mapping photonic entanglement into and out of a quantum memory. *Nature*, 2008, **452**, 67–71.
4. Clausen, C., Usmani, I., Bussières, F., Sangouard, N., Afzelius, M., de Riedmatten, H. and Gisin, N., Quantum storage of photonic entanglement in a crystal. *Nature*, 2011, **469**, 508–511.
5. Saglamyurek, E. *et al.*, Broadband waveguide quantum memory for entangled photons. *Nature*, 2011, **469**, 512–515.
6. Hosseini, M., Sparkes, B. M., Campbell, G., Lam, P. K. and Buchler, B. C., High efficiency coherent optical memory with warm rubidium vapour. *Nat. Commun.*, 2011, **2**, 1–5.

7. Hosseini, M., Campbell, G., Sparkes, B. M., Lam, P. K. and Buchler, B. C., Unconditional room-temperature quantum memory. *Nature Phys.*, 2011, **7**, 794–798.

8. Reim, K. F. *et al.*, Multipulse addressing of a Raman quantum memory: configurable beam splitting and efficient readout. *Phys. Rev. Lett.*, 2012, **108**, 263602-1–263602-5.

9. Bouwmeester, D., Ekert, A. K. and Zeilinger, A. (eds), *The Physics of Quantum Information*, Springer, New York, 2000, pp. 133–189.

10. Gisin, N., Ribordy, G., Tittel, W. and Zbinden, H., Quantum cryptography. *Rev. Mod. Phys.*, 2002, **74**, 145–195.

11. Kuzmich, A., Bowen, W. P., Boozer, A. D., Boca, A., Chou, C. W., Duan, L. M. and Kimble, H. J., Generation of nonclassical photon pairs for scalable quantum communication with atomic ensembles. *Nature*, 2003, **423**, 731–734.

12. Sherson, J. F., Krauter, H., Olsson, R.K., Julsgaard, B., Hammerer, K., Cirac, I. and Polzik, E. S., Quantum teleportation between light and matter. *Nature*, 2006, **443**, 557.

13. Knill, E., Laflamme, R. and Milburn, G. J., A scheme for efficient quantum computation with linear optics. *Nature*, 2001, **409**, 46–52.

14. Aoki, T. *et al.*, Observation of strong coupling between one atom and a monolithic microresonator. *Nature*, 2006, **443**, 671–674.

15. Dayan, B., Parkins, A. S., Aoki, T., Ostby, E., Vahala, K. and Kimble, H., A photon turnstile dynamically regulated by one atom. *Science*, 2008, **319**, 1062–1065.

16. Yang, W., Conkey, D. B., Wu, B., Yin, D., Hawkins, A. R. and Schmidt, H., Atomic spectroscopy on a chip. *Nat. Photon.*, 2007, **1**, 331–335.

17. Robinson, J. T., Chen, L. and Lipson, M., On-chip gas detection in silicon optical microcavities. *Opt. Express*, 2008, **16**, 4296–4301.

18. Spillane, S. M., Pati, G. S., Salit, K., Hall, M., Kumar, P., Beausoleil, R. G. and Shahriar, M. S., Observation of nonlinear optical interactions of ultralow levels of light in a tapered optical nanofiber embedded in a hot rubidium vapor. *Phys. Rev. Lett.*, 2008, **100**, 233602-1–233602-4.

19. Nayak, K. P., LeKien, F., Morinaga, M. and Hakuta, K., Antibunching and bunching of photons in resonance fluorescence from a few atoms into guided modes of an optical nanofiber. *Phys. Rev. A*, 2009, **79**, 021801-1–021801-4.

20. Vetsch, E., Reitz, D., Sagué, G., Schmidt, R., Dawkins, S. T. and Rauschenbeutel, A., Optical interface created by laser-cooled atoms trapped in the evanescent field surrounding an optical nanofiber. *Phys. Rev. Lett.*, 2010, **104**, 203603-1–203603-4.

21. Cregan, R., Mangan, B., Knight, J., Birks, T., Russell, P., Roberts, P. and Allan, D., Single-mode photonic band gap guidance of light in air. *Science*, 1999, **285**, 1537–1539.

22. Kato, S. and Aoki, T., Strong coupling between a trapped single atom and an all-fiber cavity. *Phys. Rev. Lett.*, 2015, **115**, 093603-1–093603-5.

23. Bures, J. and Ghosh, R., Power density of the evanescent field in the vicinity of a tapered fiber. *J. Opt. Soc. Am. A*, 1999, **16**, 1992–1996.

24. Le Kien, F., Liang, J., Hakuta, K. and Balykin, V., Field intensity distributions and polarization orientations in a vacuum-clad subwavelength-diameter optical fiber. *Opt. Commun.*, 2004, **242**, 445–455.

25. Tong, L., Lou, J. and Mazur, E., Single-mode guiding properties of sub-wavelength-diameter silica and silicon wire waveguides. *Opt. Express*, 2004, **12**, 1025–1035.

26. Le Kien, F., Balykin, V. and Hakuta, K., Light-induced force and torque on an atom outside a nanofiber. *Phys. Rev. A*, 2006, **74**, 033412-1–033412-8.

27. Le Kien, F., Gupta, S., Nayak, K. and Hakuta, K., Nanofiber-mediated radiative transfer between two distant atoms. *Phys. Rev. A*, 2005, **72**, 063815-1–0633815-11.

28. Masalov, A. and Minogin, V., Pumping of higher-order modes of an optical nanofiber by laser excited atoms. *Las. Phys. Lett.*, 2013, **10**, 075203-1–075203-6.

29. Migdall, A., Prodan, J., Phillips, W., Bergeman, T. and Metcalf, H., First observation of magnetically trapped neutral atoms. *Phys. Rev. Lett.*, 1985, **54**, 2596–2599.

30. Chu, S., Bjorkholm, J., Ashkin, A. and Cable, A., Experimental observation of optically trapped atoms. *Phys. Rev. Lett.*, 1986, **57**, 314–317.

31. Morrissey, M. J., Deasy, K., Wu, Y., Chakrabarti, S. and Nic Chormaic, S., Tapered optical fibers as tools for probing magneto-optical trap characteristics. *Rev. Sci. Inst.*, 2009, **80**, 053102-1–053102-5.

32. Russell, L., Gleeson, D. A., Minogin, V. G. and Nic Chormaic, S., Spectral distribution of atomic fluorescence coupled into an optical nanofibre. *J. Phys. B: At. Mol. Opt. Phys.*, 2009, **42**, 185006-1–185006-9.

33. Russell, L., Deasy, K., Daly, M. J., Morrissey, M. J. and Nic Chormaic, S., Sub-doppler temperature measurements of laser-cooled atoms using optical nanofibres. *Meas. Sci. Technol.*, 2012, **23**, 015201-1–015201-8.

34. Renn, M. J., Montgomery, D., Vdovin, O., Anderson, D. Z., Wieman, C. E. and Cornell, E. A., Laser-guided atoms in hollow-core optical fibers. *Phys. Rev. Lett.*, 1995, **75**, 3253–3256.

35. Ito, H., Nakata, T., Sakaki, K., Ohtsu, M., Lee, K. I. and Jhe, W., Laser spectroscopy of atoms guided by evanescent waves in micron-sized hollow optical fibers. *Phys. Rev. Lett.*, 1996, **76**, 4500–4503.

36. Dall, R. G., Hoogerland, M. D., Baldwin, K. G. H. and Buckman, S. J., Guiding of metastable helium atoms through hollow optical fibres. *J. Opt. B: Quantum Semiclassical Opt.*, 1999, **1**, 396–401.

37. Müller, D., Cornell, E. A., Anderson, D. Z. and Abraham, E. R. I., Guiding laser-cooled atoms in hollow-core fibers. *Phys. Rev. A*, 2000, **61**, 033411-1–033411-6.

38. Roberts, P. J. *et al.*, Ultimate low loss of hollow-core photonic crystal fibres. *Opt. Express*, 2005, **13**, 236–244.

39. Will, S., Atom optical experiments with ultracold sodium atoms, Diploma thesis, Johannes Gutenberg-Universität Mainz, Germany, 2006.

40. Takekoshi, T. and Knize, R. J., Optical guiding of atoms through a hollow-core photonic band-gap fiber. *Phys. Rev. Lett.*, 2007, **98**, 210404-1–210404-4.

41. Bajcsy, M. *et al.*, Efficient all-optical switching using slow light within a hollow fiber. *Phys. Rev. Lett.*, 2009, **102**, 203902-1–203902-4.

42. Slepkov, A. D., Bhagwat, A. R., Venkataraman, V., Londero, P. and Gaeta, A. L., Spectroscopy of Rb atoms in hollow-core fibers. *Phys. Rev. A*, 2010, **81**, 053825-1–053825-7.

43. Hald, J., Petersen, J. C. and Henningsen, J., Saturated optical absorption by slow molecules in hollow-core photonic band-gap fibers. *Phys. Rev. Lett.*, 2007, **98**, 213902-1–213902-4.

44. Gayraud, N., Kornaszewski, Ł. W., Stone, J. M., Knight, J. C., Reid, D. T., Hand, D. P. and MacPherson, W. N., Mid-infrared gas sensing using a photonic bandgap fiber. *Appl. Opt.*, 2008, **47**, 1269–1277.

45. Griffiths, D. J., *Introduction to Electrodynamics* (ed. Alison Reeves), Prentice-Hall India Learning Private Limited Publishers, New Jersey 07458, 1999, pp. 215–220.